UCLA-ENG--8437

UCLA-ENG--8437

DE85 003667

QUASI-THERMODYNAMIC PREDICTION OF HYDROGEN REEMISSION BEHAVIOR FROM TITANIUM FILMS

By

Y. Hirooka, R.W. Conn, D.M. Goebel

UCLA ENG 8437
PPG - 626

Oct. 1964

Printed in the United States of America

Available from:

National Technical Information Service
U.S. Department of Commerce
5285 Port Royal Road
Springfield, Virginia 22161

Price: Printed Copy
Microfiche A01

QUASI-THERMODYNAMIC PREDICTION

OF

HYDROGEN REEMISSION BEHAVIOR FROM TITANIUM FILMS

Y. Hirooka, R.W. Conn, D.M. Goebel
Department of Mechanical, Aerospace and Nuclear Engineering
and
Center for Plasma Physics and Fusion Engineering
University of California, Los Angeles
Los Angeles, California 90024

ABSTRACT

A simple method is proposed to describe the hydrogen reemission behavior from a reactive metal film in which the implanted hydrogen concentration may exceed the dilute solution range under some conditions. In this method, the conventional thermodynamic information for the metal system, namely, the phase diagram and the P-C-T (Pressure-Concentration-Temperature) relation, is used extensively to determine the reemitted hydrogen flux.

As a specific case, this method has been applied to the hydrogen reemission from a titanium film. The predicted reemission curves are found to have discontinuities in time corresponding to phase changes in the solid titanium-hydrogen system as the system proceeds to a final stationary state. In contrast, the corresponding hydrogen concentration build-up in the titanium film makes a smooth approach to the stationary state value. The effects of temperature (300-600K), titanium film thickness (10-3000 A), and incoming hydrogen flux (1.0×10^{16} - 1.0×10^{18} H atoms/cm^2•sec) on the hydrogen reemission behavior have been investigated. The length of time required to reach the stationary state changes reasonably with variation in the incoming hydrogen flux and film thickness. This characteristic transient time decreases with increasing temperature up to 600K whereas in the higher temperature range it maximizes around 700K. The stationary state hydrogen concentration is found to be independent of film thickness. In addition, the F-C-T (Flux-Concentration-Temperature) relation is derived to estimate the stationary state hydrogen concentration for a given flux and temperature.

1. INTRODUCTION

Surface characteristics of the first wall of magnetic fusion devices are widely recognized as a crucial issue affecting plasma behavior and cleanliness. Titanium carbide (TiC) is currently considered to be one of the most promising ceramics for use as a coating material to improve these wall surface characteristics. However, it has been found in recent studies [1-3] that titanium carbide is eroded either physically or chemically by hydrogen plasma bombardment. Due to this erosion, carbon is preferentially depleted so that after long exposure to the hydrogen plasma, a thin titanium layer will eventually remain on the eroded surface of the titanium carbide coatings. It is also true that titanium gettering has been used extensively for controlling impurities in many plasma confinement experiments [4-6]. During the gettering cycles, fresh titanium films are deposited and overlaid on vacuum walls of the plasma chamber. As a result, an appreciable portion (~80% [7]) of the surface area of these vacuum walls can be covered with thin titanium films. Obviously, surface chemical properties of the resultant wall are different from those of the original wall, in particular with respect to absorptivity and desorptivity for hydrogen isotopes. Clearly, chemical property changes will significantly influence the hydrogen reemission/trapping behavior at the surface.

Several experimental and numerical studies have been conducted to investigate hydrogen reemission/trapping by both reactive and non-reactive metals [8-10]. In most of these studies, hydrogen diffusion is considered to dominate the overall recycling behavior

based on the assumption that hydrogen diffusivity depends only on temperature. To solve the resultant diffusion equations, target metals are usually modelled as semi-infinite media and Sievert's law is employed as a key boundary condition. A typical example of this type of work is that carried out by Hotston and McCracken[8]. They compared their computational results with the experimental data on the trapping coefficient of 18 keV deuteron by selected reactive metals: Ti, Zr, Nb, and Pb, all in the form of 1mm thick sheets controlled to be in the temperature range, 230-1000K. Their analytical method becomes invalid when the implanted deuterium build-up in a target becomes appreciable enough to induce a change in the solid phase composition of the target metal-hydrogen system. This invalidity was actually found in the case of titanium.

Generally, Sievert's law holds as long as the dilute solution condition is satisfied for the metal-hydrogen system of interest[11]. For the titanium-hydrogen system, hydrogen concentration must be within that for the α-phase, which is a narrow solid-solution phase, to meet this condition (see fig. 1). It is likely that the α-phase range is exceeded when titanium is subjected to an intense hydrogen incoming flux. For such a case one must also consider that the hydrogen diffusivity depends upon both the hydrogen concentration and the host lattice structure for each phase[12-14]. Furthermore, titanium films having a thickness of a few microns or less should not be treated as a semi-infinite medium because the the characteristic diffusion length, $\sqrt{D}$ (D is the diffusivity), is the same order of magnitude as the film thickness at temperatures above ~500K (see table 1). Therefore, it

would be extremely difficult to apply conventional diffusion methods to the analysis of hydrogen recycling over a thin layer of a reactive metal like titanium.

These arguments clearly point to the need for a new conceptual approach to hydrogen recycling analysis which can be applied over the entire range from low to very high levels of hydrogen concentration. For this purpose, a quasi-thermodynamic concept is proposed in which thermodynamic data, specifically, the P-C-T relation and the phase transition data for the metal-hydrogen system, are used in addition to Sievert's law to determine the reemitted hydrogen flux. The approach is applied to the case of hydrogen reemission behavior from a titanium film under conditions which can occur in magnetic fusion plasma experiments.

2. THEORETICAL CONSIDERATION

2.1. Quasi-Thermodynamic Concept

Consider a metallic surface to be reacting with gaseous hydrogen of pressure, P, in an isolated system [15] held at the temperature, T, in the manner:

$$M(sol.) + H_2\ (gas) \rightleftharpoons MH_2\ (sol.). \tag{1}$$

The rate of increase in the amount of dissolved hydrogen in the metal, (dx/dt), is given by

$$\frac{dx}{dt} = V_f - V_r \tag{2}$$

where V_f and V_r are elemental reaction rates of forward and reverse directions, respectively. From the kinetic theory of gases[16],

$$V_f = \frac{\nu P}{\sqrt{2\pi mkT}} \tag{3}$$

where ν is the sticking coefficient and the rest of the symbols have their usual meaning. When this metal-hydrogen reaction system reaches its thermodynamic equilibrium, the following relations are automatically established:

$$V_f = V_r = \frac{\nu P_e}{\sqrt{2\pi mkT}} \tag{4}$$

and

$$\Delta G = \Delta G^\circ - RT\ln P_e = 0 \,. \tag{5}$$

Here, ΔG and P_e are the Gibb's free energy of the reaction and the equilibrium hydrogen pressure over the solid metal-hydrogen system, respectively.

When titanium is in contact with the hydrogen plasma, thermodynamic equilibria predicted by both eqs. (4) and (5) cannot be strictly attained because the gas-solid reaction volume is usually open for evacuation and because temperatures of gas and solid are different. However, Hirooka [17] and Malinowski [18] found that Ti-H (powder with an average particle diameter of ~5μm) and Ti-D (films with a thickness of about ~0.1μm) systems, respectively, reached quasi-thermodynamic equilibrium during the desorption process in an open reaction volume at temperatures around 550K. The quasi-thermodynamic equilibrium was such that the observed desorption rate is given by eq. (4), in which P_e is obtained from the thermodynamic pressure-concentration-temperature (P-C-T) relation for the titanium-hydrogen (deuterium) system. It is also pointed out in both these studies that the hydrogen desorption rate might not be limited by bulk diffusion because neither the powder particle size nor

the film thickness are appreciable compared with the characteristic hydrogen diffusion length at these temperatures.

Applying this quasi-thermodynamic concept to the hydrogen reemission from a reactive metal film exposed to a hydrogen plasma, the following rate equation can be obtained:

$$\frac{dx}{dt} = \left(1-b(E)\right) J_o - \frac{2\ \nu P_e(C,T)}{\sqrt{2\pi mkT}} \qquad (6)$$

where J_o is the incident hydrogen particle flux, and b(E) is the backscattering coefficient determined by the incident hydrogen energy, E. The term, C, is the average hydrogen concentration in the titanium film. The hypothetical equilibrium pressure, P_e, is a function of both C and T. These three parameters are related by the P-C-T data for the metal-hydrogen system. The reemission ratio, R, is defined as

$$R\ (t) = \frac{2\ \nu P_e(C,T)}{J\sqrt{2\pi mkT}} \qquad (7)$$

where

$$J = J_o\left(1-b(E)\right) . \qquad (8)$$

2.2. Application Criteria

It is important to point out general criteria under which the quasi-thermodynamic concept can be applied to hydrogen recycling analysis. As the primary criterion, a reactive metal film in contact with hydrogen plasma is required to be on some non-reactive substrate. Because generally non-reactive metals and alloys (Mo, W , stainless steel, TiC, etc.) have considerably lower hydrogen diffusivity and solubility compared with those for reactive metals (Ti, Nb, Zr, Pd,

etc.), one may assume no significant hydrogen flow across the film-substrate interface. The net incoming hydrogen flux deposited on the reactive metal film is thus given simply by integration of the projectile range distribution profile with respect to the film thickness.

As the second criterion, the hydrogen diffusivity expected in the reactive metal film at temperatures of interest is required to be large so that the bulk diffusion might not be the rate-limiting step of the reemission process. This means that the reactive metal film is not thick enough to be a semi-infinite diffusion medium. Due to the high hydrogen diffusivity, the initial range distribution of the implanted hydrogen will be rapidly homogenized throughout the film thickness. The resultant uniform hydrogen concentration, C, is considered to determine the phase composition of the solid metal-hydrogen system and the equilibrium pressure, $P_e(C,T)$, at a given temperature, T. Under these conditions, the incoming hydrogen energy, E, which determines the initial hydrogen distribution and the backscattering coefficient, b(E), is no longer a significant parameter. For convenience, the net incoming hydrogen flux, J, is varied as a parameter in the present analysis.

The effect of oxide impurities on the quasi-thermodynamic process should be discussed since reactive metals often form stable oxides [19] in addition to their hydrides. In hydrogen desorption experiments [17,18], the quasi-thermodynamic equilibria were established under vacuum conditions where some titanium oxides might be stable. It follows that the oxide or impurity problems are not significant in terms of establishing quasi-thermodynamic equilibrium.

Under strong reducing atmospheres such as a hydrogen plasma environment, these reactive metal oxides will be destabilized. As an example, consider the reducing reaction of TiO_2 by thermal neutral atomic hydrogen, H, which is one of the constituents, in the edge plasma region of magnetic fusion devices [20]:

$$TiO_2 + 4H = Ti + 2H_2O, \quad \Delta G^\circ \tag{9}$$

where ΔG° is the standard Gibb's free energy of the reaction. Using the data collected in JANAF [19] yields

$$-361 \lesssim \Delta G^\circ \lesssim -251 \text{ (kJ)}$$

for the temperature range 400-1000K. These large negative values of ΔG° suggest that the reaction (9) is likely to occur under conditions where low water vapor pressure is expected. As a result, we assume that quasi-thermodynamic equilibrium will be established during desorption because of the destabilization of the oxide layer by the incident hydrogen plasma flux.

Finally, lattice defects such as vacancies and voids can alter the ordinary hydrogen mobility and solubility in metals. It was found for the Ti-H system[21,22] that fast neutron (E > 1MeV) radiation damage increased the hydrogen absorption rate by 40-50% and the hydrogen solubility by a few percent, in the temperature range 723-893K. An altered P-C-T relation was also reported for the neutron irradiated Ti-H system. In the case of 310 stainless steel (310SS)[23], the neutron radiation damage was found to reduce the hydrogen diffusivity by 60% and the hydrogen solubility by two orders of magnitude over the temperature range, 453-833K. Wilson and Baskes[10] attempted to explain the delayed deuterium desorption from 316SS by adding a term to

account for the effect of radiation-induced trapping sites to the diffusion equation. To apply the quasi-thermodynamic concept to the case where radiation damage due to the incident hydrogen plasma particles is significant, one should prepare the suitable P-C-T and phase transition data for the damaged metal-hydrogen system.

In the case of titanium, the criteria for applicability of the quasi-thermodynamic approach will be satisfied in three important cases: (1) a thin titanium film is formed on the eroded surface of TiC or TiO_2 after prolonged exposure to a hydrogen plasma; (2) thin titanium films are produced directly, as in the case of gettering the walls of plasma confinement chambers. Structural materials for the chamber walls are generally non-reactive metals such as stainless steel; (3) a titanium film imbedded with tritium is used as a solid target for a deuteron beam in a neutron source facility [24]. A copper substrate is employed for this purpose. For this case one must consider the effect of the radiation damage due to both deuteron and neutron on the themodynamic properties of the Ti-D, T system.

3. RESULTS AND DISCUSSION

3.1. Thermodynamic Data Treatment

The rate equation (6) is of the form which can be numerically solved by the Runge-Kutta method. To obtain the numerical solution, it is necessary to interpolate the conventional P-C-T data for the Ti-H system so that when the hydrogen concentration, C, and the temperature, T, are specified, the equilibrium hydrogen overpressure, $P_e(C,T)$, can be determined uniquely.

From the data reported by McQuillan[24], the equilibrium hydrogen pressures for the α and β phases are given by

$$P_\alpha(C,T) = kC^2 \exp(Q_0/RT) \tag{10}$$

and

$$P_\beta(C,T) = kC^2 \exp(\lambda C^\mu) \exp\{Q_0(1-\eta C^\xi)/RT\}, \tag{11}$$

respectively. Values of the parameters are given in ref. [25]. Although the corresponding expression for the (α+β) phase is not available, it is reasonable to assume that the equalibrium hydrogen pressure for this two-phase region is given by a linear relation determined by two phase boundary points:

$$P_{\alpha+\beta}(C,T) = \frac{P_\alpha(C_a(T),T)-P_\beta(C_b(T),T)}{C_a(T)-C_b(T)}(C-C_b(T))+P_\beta(C_b(T),T) \tag{12}$$

where $C_a(T)$ and $C_b(T)$ are the hydrogen concentration at the α → (α+β) and the (α+β) → β phase boundaries, respectively, both of which depend on temperature. For the (α+γ) and (β+γ) phases, the expressions

$$P_{\alpha+\gamma}(C,T) = P_\alpha(C_a(T),T) \tag{13}$$

and

$$P_{\beta+\gamma}(C,T) = P_\beta(C_c(T),T) \tag{14}$$

can be obtained from the phase rule [11], where $C_c(T)$ is the hydrogen concentration at the β → (β+γ) phase boundary. Finally, for the γ-phase (the hydride phase of TiH_2), the following relation is used under the assumption that the equilibrium hydrogen pressure approaches to P_{sat} of 101.3kPa(1 atm) at the saturation hydrogen concentration, C_{sat}, of 63.3 at %[25]:

$$\log[P_\gamma(C,T)] = \frac{\log[P_{\beta+\gamma}(C_d(T),T)] - \log[P_{sat}]}{\log[C_d(T)] - \log[C_{sat}]}(\log[C]-\log[C_{sat}])+\log[P_{sat}] \tag{15}$$

where $C_d(T)$ is the hydrogen concentration at the $(\alpha+\gamma) \rightarrow \gamma$ and the $(\beta+\gamma) \rightarrow \gamma$ phase boundaries.

The phase boundary data are also modified so that when the temperature, T, is specified, the phase boundary hydrogen concentrations, $C_a(T)$, $C_b(T)$, $C_c(T)$ and $C_d(T)$ can be determined. At temperatures above ~600K, these phase transition data have well been established over the wide hydrogen concentration range from 0 to 63.3 at%[24]. For the lower temperature range, the $\alpha \rightarrow (\alpha+\gamma)$ phase boundary has been reported in the low hydrogen concentration range, 0.05-8.4 at%[26]. It was recognized in a previous experiment [17] that under quasi-thermodynamic conditions, the initial peak of the hydrogen desorption rate is followed by the plateau level at temperatures 523-603K. This suggests that there must be the $(\alpha+\gamma) \rightarrow \gamma$ phase boundary somewhere near a hydrogen concentration of ~50 at % in this temperature range. However, the $(\alpha+\gamma) \rightarrow \gamma$ phase boundary has been reported only at temperatures below 400K[14]. In the present study, these experimental phase transition data points shown in fig. 1 are interpolated by the Lagrange method while some points were determined by likely extrapolation of these reported data. This arrangement of phase transition data allows us to obtain a wide range of P-C-T information for the Ti-H system. The resultant semi-theoretical P-C-T relation at temperatures 300-600K is shown in fig. 2.

3.2. Kinetic Data Treatment

As one can see in eq. (6), the reemitted hydrogen flux strongly depends on the hydrogen sticking coefficient, ν. Surveying

conventional data[27-29], one finds that the sticking coefficient for hydrogen on titanium has been measured at temperatures below ~350K. There is essentially no data for ν reported in the temperature range where hydrogen reemission is of interest in this paper. Earlier experimental data for hydrogen desorption rates from TiH_2 powder[17] have been compared with theoretical values determined from the second term of eq. (6). The sticking coefficient is roughly estimated to be 2×10^{-4} for the solid Ti-H system in the (α+γ)-phase at temperatures ~550K. This sticking coefficient value is an order of magnitude below the value of 2×10^{-3} reported at 348K[28]. This discrepency is not surprising because smaller sticking coefficients are generally found as the temperature increases.

The two sticking coefficients obtained at 348 and 550K can be interpreted in terms of the Arrhenius relation:

$$\nu(T) = 3.3 \times 10^{-6} \exp\,(18.5\ [kJ/mol]/RT). \qquad (16)$$

The negative activation energy in this kinetic expression is not unreasonable since hydrogen absorption by titanium is an exothermic process. The sticking coefficient is assumed to be independent of hydrogen concentration for simplicity. The value given by eq. (16) is used in the present analysis, unless otherwise specified.

3.3. Hydrogen Reemission

A computer program has been developed to solve eq. (6) using the thermodynamic and kinetic data treatment just described. We have then specifically examined the problem of hydrogen reemission from a titanium film under conditions which can occur in typical magnetic

fusion confinement experiments. These conditions include the hydrogen plasma discharge period, the operating vacuum wall temperature, and the net incoming hydrogen flux. The simulated plasma discharge period is set at 2.0 seconds, unless otherwise specified, in the present study. The initial hydrogen concentration in the titanium film is assumed to be zero for convenience. The first applicability criterion of section 2.2 is assumed to be satisfied.

Under these conditions, the temperature dependence of the hydrogen reemission and the hydrogen concentration build-up behavior is investigated first for the case where the net incoming hydrogen flux is set at 1×10^{17} H atoms/cm^2•sec and the titanium film thickness is 100 Å. From the hydrogen diffusivity data cited in table 1, the second applicability criterion of section 2.2 is satisfied for this titanium film thickness when the temperature is above ~300K. Because the phase transition behavior of the solid titanium-hydrogen system is significantly different above and below about 600K, the hydrogen reemission behavior will be shown separately for these two temperature ranges.

The predicted behavior of the hydrogen reemission and the hydrogen concentration build-up in the titanium film in the low temperature range, 300-500K are shown in figs. 3-a and b, respectively, and the data obtained are summarized in table 2. One can see that the reemission ratio curves show a characteristic discontinuous behavior: an initial increase, a plateau level and an abrupt increase to reach the stationary state[15], within the given discharge period. In contrast, the hydrogen concentration curves show a smooth approach

to the respective stationary values, C_s. At this stationary state, the reemission ratio, R, is held at unity because the hydrogen concentration is time-independent. When the temperature becomes higher, the estimated value of C_s decreases. This temperature dependence of C_s is consistent with the thermodynamic property of the titanium-hydrogen system in that a higher temperature favors lower hydrogen solubility. Because the values of C_s are those for the γ-phase (titanium hydride: TiH_2) in this temperature range, the solid titanium-hydrogen system must undergo two phase changes, namely $\alpha \rightarrow (\alpha+\gamma) \rightarrow \gamma$ until the stationary state is attained. The characteristic breaks seen on the reemission curves can be found to correspond to these phase changes. Obviously, these high stationary hydrogen concentrations far exceed the dilute solution range where Sievert's law can hold. This evaluation qualitatively agrees with recent experimental results which find that titanium samples exposed to the hydrogen plasma contain a large amount of hydrogen[7,30,31]. The time required to reach the stationary state, τ, decreases as the temperature increases. This temperature dependence of τ is consistent with that predicted by conventional diffusion methods[8,9]. After the simulated plasma discharge period is over, the reemission ratio curves show the simple desorption rates, D, determined from the relation, $D = R \cdot J$. As shown in previous work[17], it will take 1-2 hours before the hydrogen concentration returns to that for the α-phase at these temperatures. As such, high temperature baking appears to be necessary to more rapidly recover the hydrogen trapping capacity of the titanium film. This will be quantitative shown later.

The corresponding results obtained for the high temperature range are shown in figs. 4-a and b, and table 2. There are more breaks in the remission curves than seen earlier. This is due to the frequent phase transitions that occur in this temperature range. At 600K, for example, four distinct phase changes occur as the hydrogen concentration proceeds to the stationary value, C_s. The estimated value of C_s decreases with increasing temperature and above 700K, the γ-phase is no longer reached. This is consistent with the hot-wall concept proposed by Keller et al.[30] that the high temperature operation of titanium-gettered walls will serve to avoid surface flaking due to γ-phase hydride precipitation. Unlike our finding in the low temperature range, the time required to reach the stationary state seems to maximize at ~700K. It is difficult to plausibly interpret the overall temperature dependence (300-600K) of τ with a simple kinetic concept. This anomalous temperature dependence should be due to the significant difference in the phase transition behavior in the two temperature ranges. After the discharge period, the implanted hydrogen is released quite rapidly in the high temperature range (see the C_f values in table 1). Note that the hydrogen desorption curves show characteristic discontinuous breaks similar to those found on the approach to the stationary state during hydrogen bombardment.

These discontinuous breaks are found in existing experimental data on deuterium reemission curves for titanium oxide and carbide coatings at temperatures, 300-775K[32]. However, this behavior has not been explicitly pointed out or explained. Also, the anomalous

temperature dependence of τ similar to that described above was observed for titanium oxide coatings in this same series of experiments but was treated as being exceptional data within the overall catalog of data reported for other low-Z coating materials. [32]

As suggested by eq. (9), the surface layer of titanium oxide coatings might be destabilized by the D_2^+ bombardment up to a fluence of 10^{17}-10^{18} D atoms/cm^2. Therefore, a plausible interpretation of the data of Erents [32] can be developed by assuming that a quasi-thermodynamic equilibrium was established in the deuterium reemission process from the destabilized surface layer of titanium oxide. Accordingly, the retained deuterium concentration within this surface layer is estimated to be 40-50 at% for the stationary states at 575K and 775K because four discontinuities can be seen in the respective reemission curves. It is unfortunate that little attention was given to the hydrogen concentration build-up in the target materials during these conventional reemission experiments.

To simulate the case where the titanium film thickness changes, hydrogen reemission behavior as a function of titanium film thickness has been investigated. The titanium film thickness is varied in the range from 10 to 3000 A. To meet the hydrogen diffusivity criterion over the wide thickness range, the temperature is set at 500K (see table 1). The simulated plasma discharge period and the net incoming hydrogen flux are assumed to be 3.0 sec and 1.0×10^{17} H atoms/cm^2.sec, respectively. The results are shown in figs. 5-a, b and table 3. The time required to reach the stationary state, τ, increases with increasing titanium film thickness. However, the stationary hydrogen

concentration, C_s is found to be independent of the titanium film thickness. In the cases where the titanium film thickness is 1000 and 3000 A, the reemission ratios at the end of the simulated plasma discharge are identical although the corresponding hydrogen concentrations are different. This can be understood by the fact that the solid Ti-H systems in both cases is in the $(\alpha+\gamma)$-phase where the hydrogen equilibrium pressure determining the reemitted flux is independent of the hydrogen concentration.

Finally, the effect of the net incoming hydrogen flux on the reemission behavior is examined. The film thickness and the temperature are set 100 A and 500K, respectively. The results are shown in figs. 6-a and b, and table 4. When the net incoming hydrogen flux increases, the estimated value of τ decreases while the stationary hydrogen concentration becomes higher. One sees that a larger concentration decrease after the plasma discharge, (C_s-C_f), is favored by a higher stationary hydrogen concentration in the γ-phase until the $(\alpha+\gamma)$-phase is reached.

These results can best be understood as follows: At the stationary state,

$$P_e(C_s,T) = J\sqrt{2\pi mkT}/2\nu(T) \qquad (17)$$

is established from eq. (6). This relation means that when the net incoming hydrogen flux, J, and the temperature, T, are specified, the equilibrium hydrogen pressure, $P_e(C_s,T)$, is determined. It follows that the stationary state hydrogen concentration, C_s, can be obtained from the P-C-T relation shown in fig. 2. As such, it is reasonable that the stationary hydrogen concentration is independent of the film

thickness. Using eq. (17), the F-C-T (Flux-Concentration-Temperature) relation is derived and the result is shown in fig. 7. This F-C-T relation allows us to predict the stationary state hydrogen concentration in a titanium film of any thickness when the net incoming hydrogen flux and temperature are specified.

4. CONCLUSION

A simple quasi-thermodynamic theory is developed to predict the hydrogen reemission behavior from a reactive metal film. To deal with cases where the implanted hydrogen concentration exceeds the range of validity for Sievert's law, the thermodynamic P-C-T relation is combined with the phase transition data to determine the reemitted hydrogen flux. The applicability criteria for this method has been described in detail.

As an example, the method has been applied to hydrogen reemission from a titanium film. The predicted reemission curves show characteristic discontinuities until the stationary state is attained. These breaks have been found to correspond to the phase transitions of the solid Ti-H system along with the hydrogen concentration change. Unlike the reemission behavior, the hydrogen concentration build-up makes a smooth approach to the stationary value. The stationary hydrogen concentration is found to be independent of the titanium film thickness and to decrease with increasing temperature. The F-C-T relation has been derived and used to evaluate the stationary hydrogen concentration for a given temperature and incoming hydrogen flux. The time required to reach the stationary state, τ, shows reasonable

behavior with variation in the net incoming hydrogen flux. The time required to reach the stationary state, τ, shows reasonable behavior with variation in the net incoming hydrogen flux and film thickness. An anomalous temperature dependence of τ is also predicted. These predictions have been found to qualitatively agree with some reported experimental data for the titanium-plasma interactions.

In summary, the quasi-thermodynamic method can be applied to hydrogen reemission analysis for reactive metal films so long as the applicability criteria are met and were the required thermodynamic information available. To fully examine the validity of this method, further experimental investigation is greatly anticipated.

ACKNOWLEDGEMENT

Illuminating discussions with Drs. L. Keller, and A.K. Prinja (UCLA) are sincerely appriciated. Important suggestions by Drs. K. Sone and M. Kinoshita (JAERI) are also acknowledged. This work is supported by the United States Department of Energy, Office of Fusion Energy under contracts DOE-EY24-PAER52104 and DE-AT03-80ER52062.

AT03-84ER52104

REFERENCES

[1] A.A. Haasz. P.C. Stangeby and O. Auciello, J. Nucl. Mater. 111 & 112, 757 (1982).

[2] H. Tanaka, K. Saiki, S. Otani, A. Koma and S. Tanaka, Ibid. 116, 317 (1983).

[3] S. Sukenobu and S. Gomay, J. Vac. Sci. & Technol. -A 1, 920, (1983).

[4] R.J. Taylor, J. Nucl. Mater. 76 & 77, 41 (1876).

[5] L. Keller, C.N.J. Wagner, F. Schwirzke, and R.J. Taylor, Ibid. 107, 104 (1982).

[6] W.L. Pickles, A.K. Chargin, R.P. Drake, A.L. Hunt, D.D. Lang, J.J. Murphy, P. Poulsen, T.C. Simonen, T.H. Batzer, T.P. Stack and R.L. Wong, J. Vac. Sci. & Technol. 20, 1177 (1982).

[7] W.L. Hsu, R. Bastasz. W. Bauer, M.E. Malinowski and B.E. Mills, SAND83-8843.

[8] E.S. Hotston and G.M. McCracken, J. Nucl. Mater. 68, 277 (1977).

[9] K. Erents and G.M. McCracken, Brit. J. Appl. Phys. ser. 2, 2, 1397 (1969).

[10] K.L. Wilson and M.J. Baskes, J. Nucl. Mater. 76 & 77, 291 (1978).

[11] D.R. Gaskell, Introduction to Metallurgical Thermodynamics (McGraw-Hill, 1973), Chap. 13.

[12] T.P. Papazolou and M.T. Hepworth, Trans. Met. Soc. AIME 242, 662 (1968).

[13] R.J. Wasilewski and G.L. Kehl, Metallurgia 50, 225 (1959).

[14] C. Korn and D. Zamir, J. Phys, Chem. Solids 31, 469 (1970).

[15] I. Prigogine, Introduction to Thermodynamics of Irreversible processes, 2nd ed. (John Wilen & Sons, 1961), Chaps. 1, 5 and 6.

[16] S. Dashman, Scientific Foundation of Vacuum Technique, 2nd ed. (Wiley, 1962) Chap. 8.

[17] Y. Hirooka, Vac. Sci. & Technol. -A 2, 16 (1984).

[18] M.E. Malinowski. J. Nucl. Mater. 85 & 86, 957 (1979).

[19] JANAF Thermochemical Tables (2nd ed.), Nat. Stand. Ref. Data Ser., Nat. Bur. Stand. (1971).

[20] G.M. McCracken and P.E. Stott, Nucl. Fusion 19, 889 (1979).

[21] Y. Hirooka, Ph.D Thesis (Osaka Univ., Japan, 1961), Chap. 4.

[22] M. Miyake, Y, Hirooka, H. Shinmura, Y. Yamanaka, T. Sano and H. Higashiguchi, J. Nucl. Mater. 103 & 104, 477 (1981).

[23] N.R. Quick, Ph.D Thesis (Cornell Univ., USA, 1976), Chap. 3.

[24] R. Booth and H.H. Barschall, Nucl. Instrum. Methods 99, 1, (1972).

[25] A.D. McQuillan, Proc. Royal Soc., London A204, 309 (1950).

[26] G.A. Lenning, C.M. Craighead and R.I. Jaffee, Trans. AIME 200, 367 (1954).

[27] D.J. Harra, J. Vac. Sci. & Technol. 13, 471 (1976).

[28] J.W. Reichardt, ibid. 9, 548 (1972).

[29] M.E. Malinowski, J. Nucl. Mater. 63, 386 (1976).

[30] L. Keller, L. Oren, R.J. Taylor, F. Schwirzke, R.F. Bunshah and C.N.J. Wagner, ibid. 111 & 112, 493 (1982).

[31] J. Roth, W. Eckstein and Bohdansky, Radiat. Eff. 48, 231 (1980).

[32] S.K. Erents, J. Nucl. Mater. 111 & 112, 590 (1982).

FIGURE CAPTIONS

Fig.1: The phase diagram of the titanium-hydrogen system. The data shown by symbols of ●,▲, and ■ are after McQuillan[25], Lenning et al.[26], and Korn and Zamir [14], respectively. The points shown by the symbol of ◐ are assumed by a likely extrapolation of these reported data.

Fig.2: The semi-theoretical P-C-T relation for the titanium-hydrogen system in the temperature range from 300 to 600K.

Fig.3: The temperature effect (300-550K) on the reemission behavior (a), and the corresponding hydrogen concentration change (b). The titanium film thickness of 100 Å and the net incoming hydrogen flux of 1.0×10^{17} H atoms/cm^2.sec are assumed.

Fig.4: The temperature effect (600-800K) on the reemission behavior (a), and the corresponding hydrogen concentration change (b). The titanium film thickness and the net incoming hydrogen flux are assumed to be identical to those for the low temperature range.

Fig.5: The film thickness effect (10-3000 Å) on of the reemission behavior (a), and the corresponding hydrogen concentration change (b). The temperature of 500K and the net incoming hydrogen flux of 1.0×10^{17} H atoms/cm^2.sec are assumed.

Fig.6: The incoming flux effect (1.0×10^{16} - 1.0×10^{18} H atoms/cm^2•sec) on the reemission behavior (a), and the corresponding hydrogen concentration change (b). The temperature of 500K and the titanium film thickness of 100 Å are assumed.

Fig.7: The F-C-T relation for the titanium film - hydrogen plasma system in the temperature range from 300 to 600K.

Table 1. Characteristic diffusion length estimated from representative hydrogen diffusivity data for titanium.

Temperature (K)	$\sqrt{D_1 t_0}^*$ (μm)	$\sqrt{D_2 t_0}^*$ (μm)	$\sqrt{D_3 t_0}^*$ (μm)
100	4.71×10^{-14}	1.25×10^{-11}	6.32×10^{-6}
200	6.32×10^{-6}	7.27×10^{-5}	3.28×10^{-2}
300	2.42×10^{-3}	1.31×10^{-2}	5.16×10^{-1}
400	5.28×10^{-1}	1.76×10^{-1}	2.14
500	3.35×10^{-1}	8.34×10^{-1}	4.92
600	1.15	2.35	8.59
700	2.77	4.96	4.0
300	5.37	8.63	17.3
900	8.98	13.3	21.8
1000	13.6	18.8	26.3

*) $D_1 = 3.0\times10^{-2}$ exp (-61.5 [kJ/mol]/RT) [cm^2/sec] (for the α-phase [12]).
$D_2 = 1.8\times10^{-2}$ exp (-51.8 [kJ/mol]/RT) [cm^2/sec] (for the α-phase [13]).
$D_3 = 1.95\times10^{-3}$ exp (-27.8 [kJ/mol]/RT) [cm^2/sec] (for the β-phase [13]).
t_0 = 0.1 [sec].

Table 2. Temperature effect on the hydrogen reemission behavior.*

Temperature (K)	Reemission behavior data τ (sec)	R	C_s (at%)	C_f** (at%)	Phase transition data $C_a(T)$ (at%)	$C_b(T)$ (at%)	$C_c(T)$ (at%)	$C_d(T)$ (at%)
300	0.958	1.0	62.3	61.8	0.0216	-	-	59.9
350	0.952	1.0	61.4	60.4	0.0616	-	-	57.5
400	0.942	1.0	60.4	58.9	0.172	-	-	55.3
450	0.930	1.0	58.5	56.0	2.42	-	-	53.3
500	0.912	1.0	56.8	53.5	3.67	-	-	51.2
550	0.898	1.0	54.7	50.4	5.35	-	-	48.2
600	0.860	1.0	52.4	46.8	7.94	37.6	36.9	47.8
650	0.956	1.0	52.3	33.8	7.94	34.5	44.5	50.3
675	1.15	1.0	52.3	21.9	7.94	33.1	46.2	51.6
700	1.66	1.0	45.3	3.56	7.94	31.5	47.6	52.8
725	1.43	1.0	40.3	1.25	7.94	29.4	48.2	53.8
750	1.26	1.0	35.4	0.661	7.94	27.8	46.7	55.0
800	1.36	1.0	26.5	0.273	7.94	25.3	49.0	56.7

*) The titanium film thickness and the net hydrogen incoming flux are set at 100 Å and 1.0×10^{17} H atoms/cm^2.sec, respectively.

**) The value C_f is the hydrogen concentration at t = 4.0 sec (2.0 sec after the plasma discharge is over).

Table 3. Titanium film thickness effect on the hydrogen reemission behavior.*

Thickness (Å)	Reemisssion behavior data			
	τ (sec)	R	C_s (at%)	C_f (at%)
10	0.090	1.0	56.8	52.4
30	0.274	1.0	56.8	53.2
100	0.912	1.0	56.8	54.0
300	2.77	1.0	56.8	54.7
1000	(3.0)	(2.96×10^{-4})	~57**(34.7)	34.7
3000	(3.0)	(2.96×10^{-4})	~57**(15.0)	15.0

*) The net incoming hydrogen flux and the temperature are set at 1.0×10^{17} H atoms/cm^2.sec and 500K, respectively. The simulated plasma discharge period is assumed to be 3.0 sec.

**) The stationary state hydrogen concentration values are estimated from the F-C-T relation.

***) The values in parentheses are those at the end of the plasma discharge.

Table 4. Net incoming hydrogen flux effect on the hydrogen reemission behavior*.

Net Hydrogen Flux (H atoms/cm^2•sec)	Reemisssion behavior data			
	τ (sec)	R	C_s (at%)	C_f (at%)
1.0×10^{16}	(2.0)	(2.95×10^{-3})	-54**(26.1)	26.0
3.0×10^{16}	(2.0)	(1.37×10^{-3})	-55**(51.4)	51.4
1.0×10^{17}	0.912	1.0	56.8	53.5
3.0×10^{17}	0.324	1.0	57.6	53.5
1.0×10^{18}	0.100	1.0	56.5	53.5

*) The titanium film thickness and the temperature are set at 100 A and 500K, respectively.

**) The stationary hydrogen concentration values are estimated from the F-C-T relation.

***) The values in parentheses are those at the end of the plasma discharge.

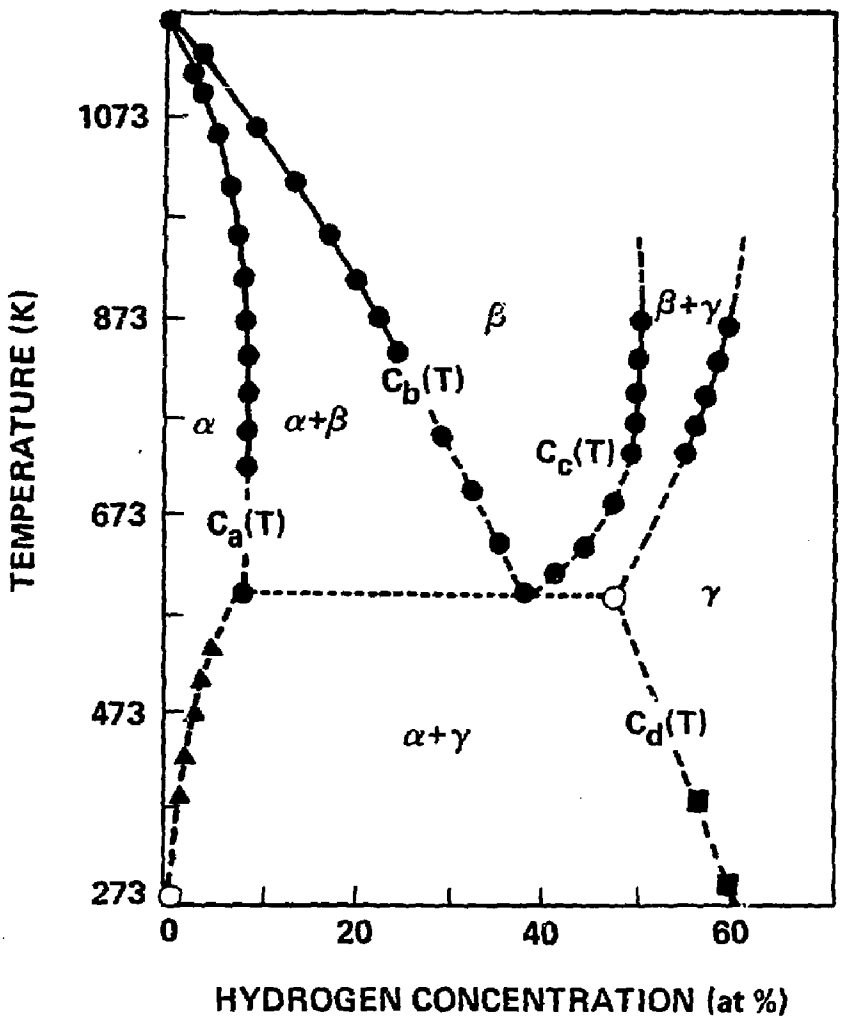
1073
873
673
473
273
0
20
40
60
TEMPERATURE (K)
HYDROGEN CONCENTRATION (at %)
α
α+β
β
β+γ
γ
α+γ
C_a(T)
C_b(T)
C_c(T)
C_d(T)

Fig. 1

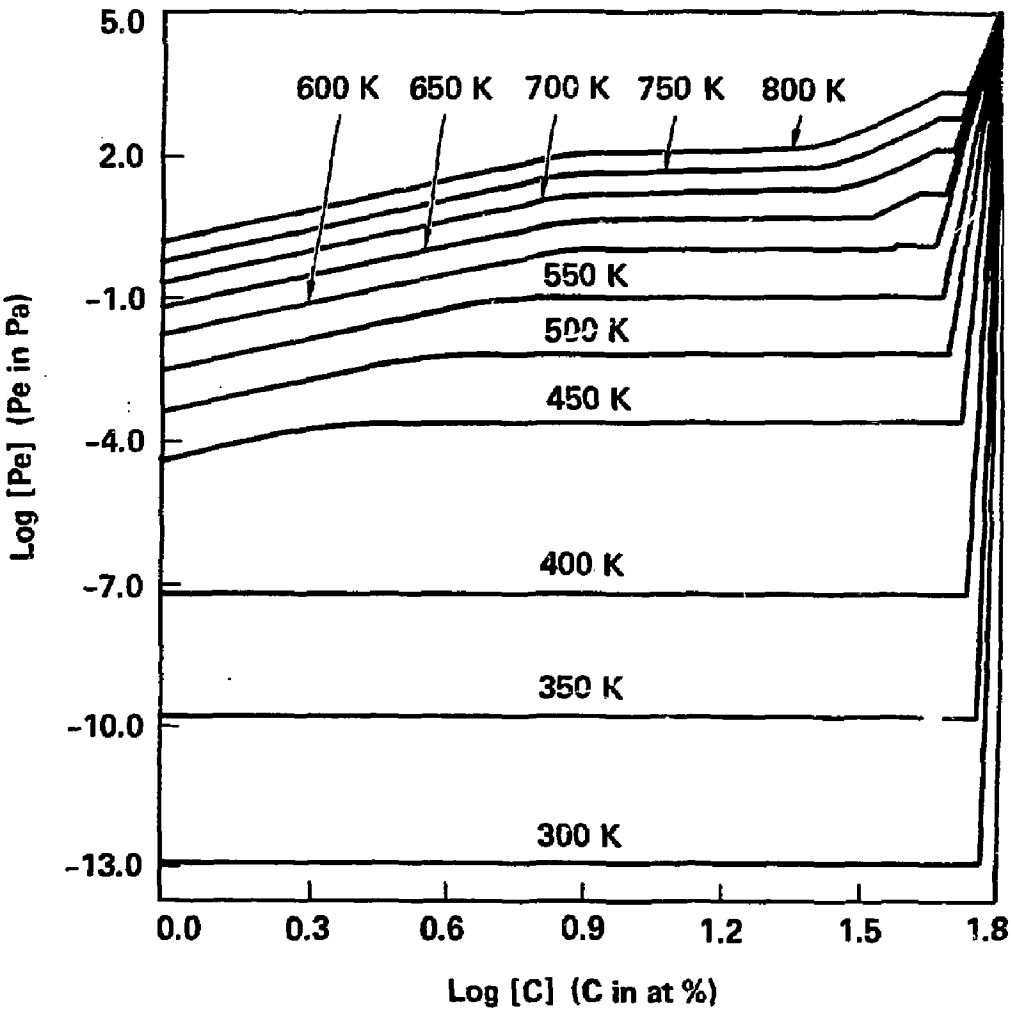
5.0
2.0
-1.0
-4.0
-7.0
-10.0
-13.0
600 K
650 K
700 K
750 K
800 K
550 K
500 K
450 K
400 K
350 K
300 K
0.0
0.3
0.6
0.9
1.2
1.5
1.8
Log [Pe] (Pe in Pa)
Log [C] (C in at %)

Fig. 2

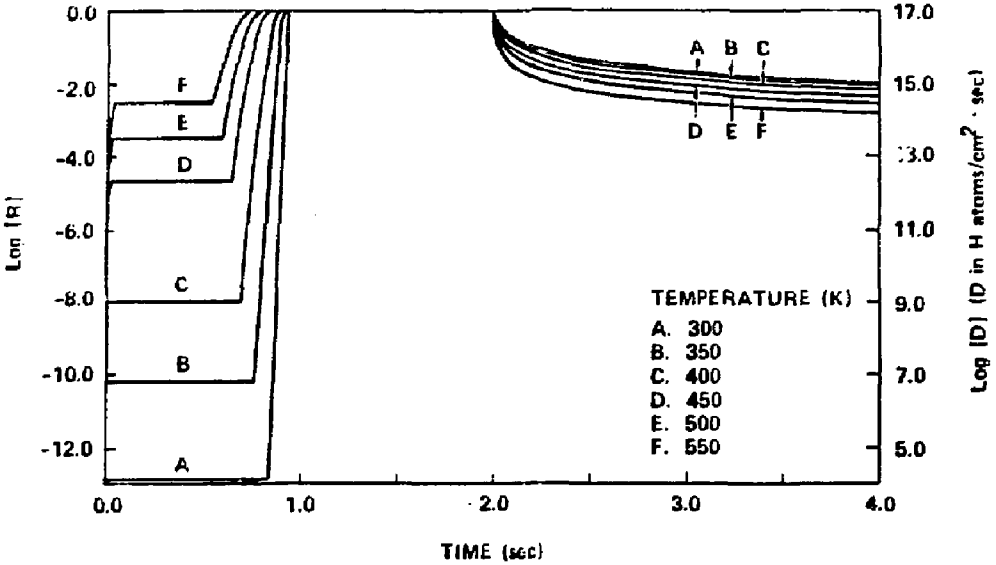
0.0
-2.0
-4.0
-6.0
-8.0
-10.0
-12.0
Log [R]
F
E
D
C
B
A
A B C
D E F
17.0
15.0
13.0
11.0
9.0
7.0
5.0
Log [D] (D in H atoms/cm² · sec)
TEMPERATURE (K)
A. 300
B. 350
C. 400
D. 450
E. 500
F. 550
0.0
1.0
2.0
3.0
4.0
TIME (sec)

Fig. 3(a)

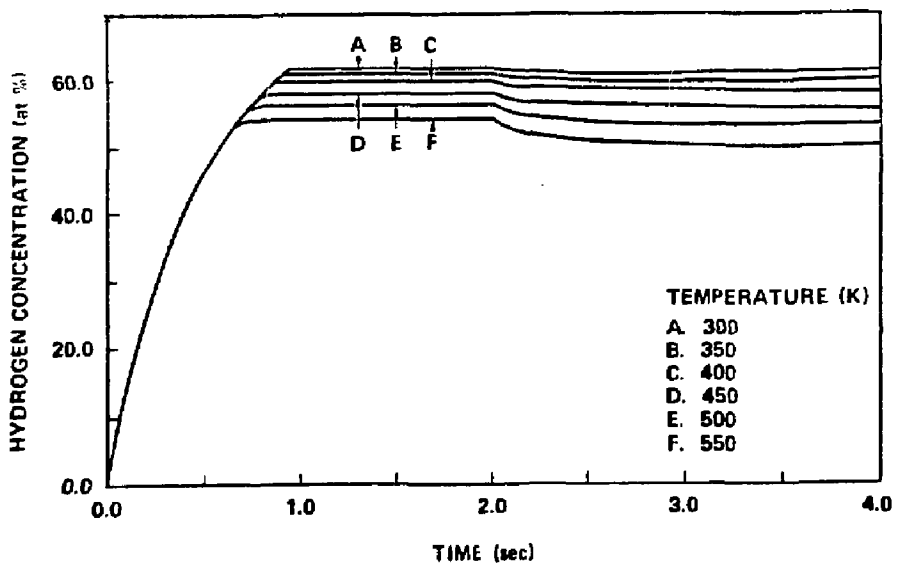
HYDROGEN CONCENTRATION (at %)
60.0
40.0
20.0
0.0
A B C
D E F
TEMPERATURE (K)
A. 300
B. 350
C. 400
D. 450
E. 500
F. 550
0.0
1.0
2.0
3.0
4.0
TIME (sec)

Fig. 3(b)

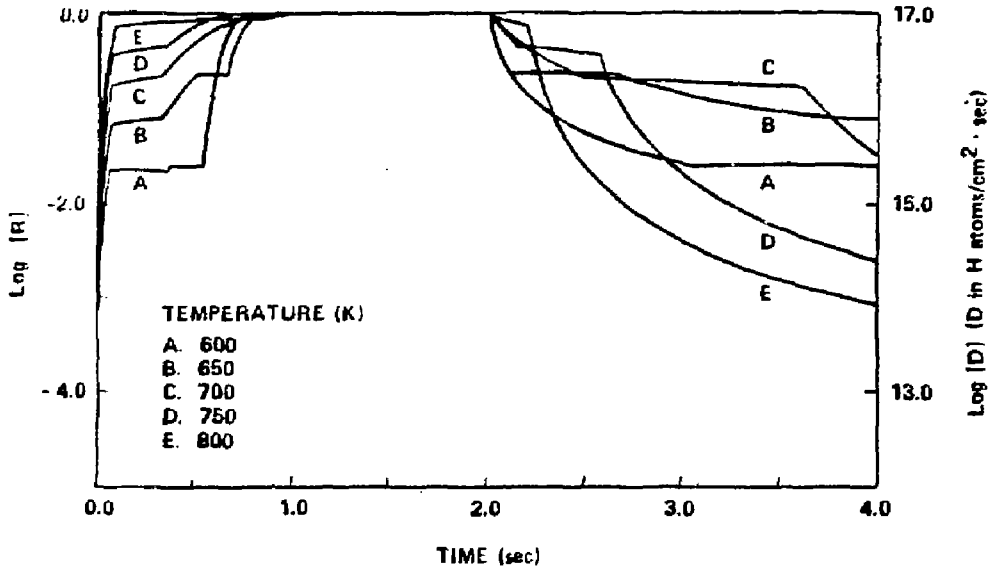
0.0
-2.0
- 4.0
Log [R]
17.0
15.0
13.0
Log [D] (D in H atoms/cm^2 · sec)
TEMPERATURE (K)
A. 600
B. 650
C. 700
D. 750
E. 800
0.0
1.0
2.0
3.0
4.0
TIME (sec)

Fig. 4(a)

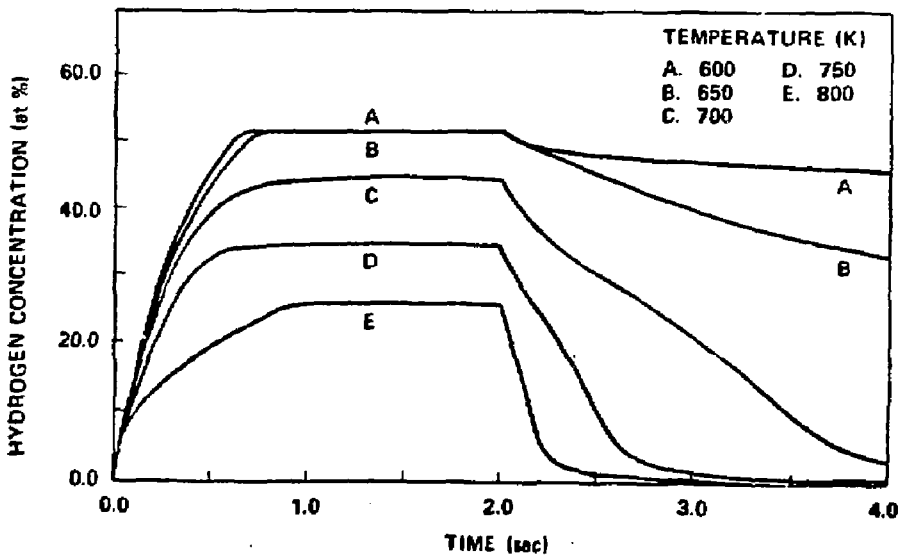
HYDROGEN CONCENTRATION (at %)
60.0
40.0
20.0
0.0
TEMPERATURE (K)
A. 600
B. 650
C. 700
D. 750
E. 800
0.0
1.0
2.0
3.0
4.0
TIME (sec)

Fig. 4(b)

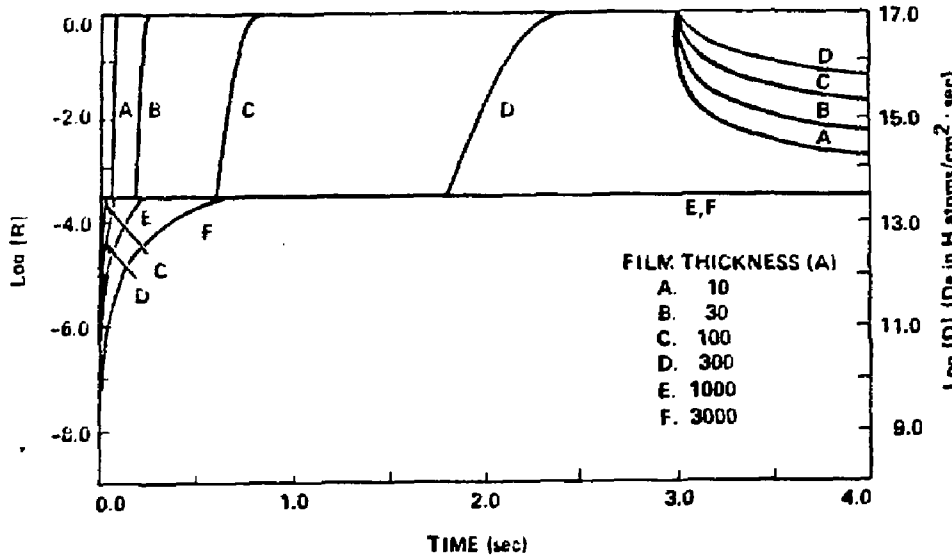
0.0
-2.0
-4.0
-6.0
-8.0
Log [R]
17.0
15.0
13.0
11.0
9.0
Log [D] (De in H atoms/cm^2 · sec)
A
B
C
D
E
F
E,F
FILM THICKNESS (A)
A. 10
B. 30
C. 100
D. 300
E. 1000
F. 3000
0.0
1.0
2.0
3.0
4.0
TIME (sec)

Fig. 5(a)

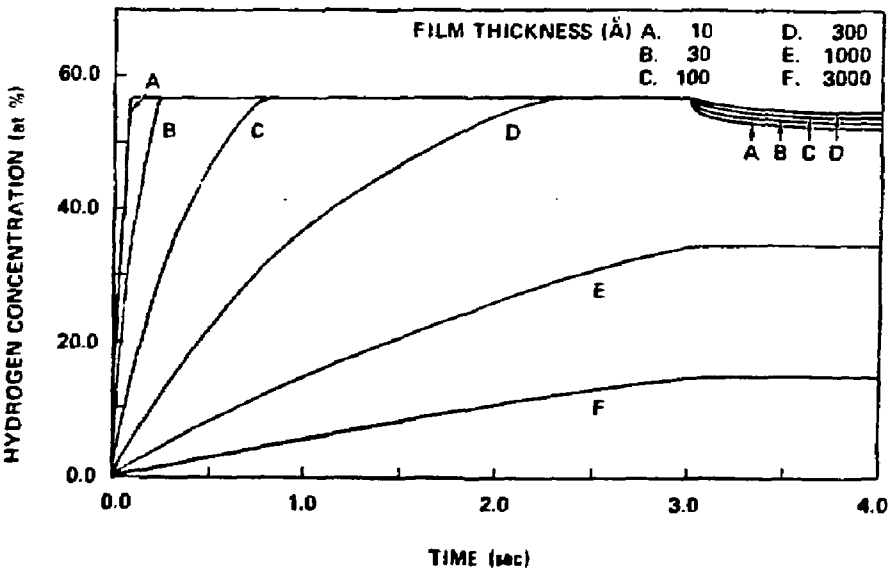
FILM THICKNESS (Å) A. 10
B. 30
C. 100
D. 300
E. 1000
F. 3000
HYDROGEN CONCENTRATION (at %)
60.0
40.0
20.0
0.0
A
B
C
D
E
F
A B C D
0.0
1.0
2.0
3.0
4.0
TIME (sec)

Fig. 5(b)

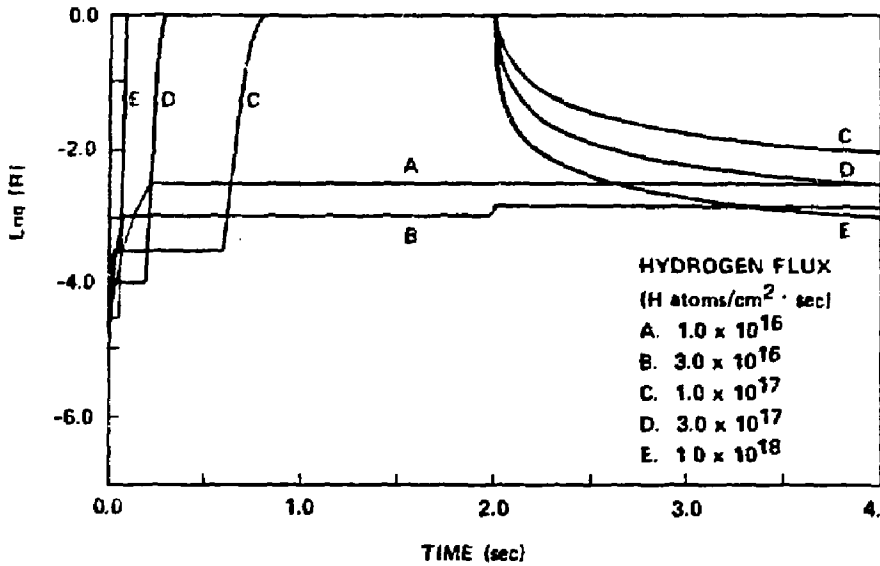
0.0
-2.0
-4.0
-6.0
Log [R]
E
D
C
A
B
C
D
E
HYDROGEN FLUX
(H atoms/cm^2 · sec)
A. 1.0 x 10^{16}
B. 3.0 x 10^{16}
C. 1.0 x 10^{17}
D. 3.0 x 10^{17}
E. 1.0 x 10^{18}
0.0
1.0
2.0
3.0
4.0
TIME (sec)

Fig. 6(a)

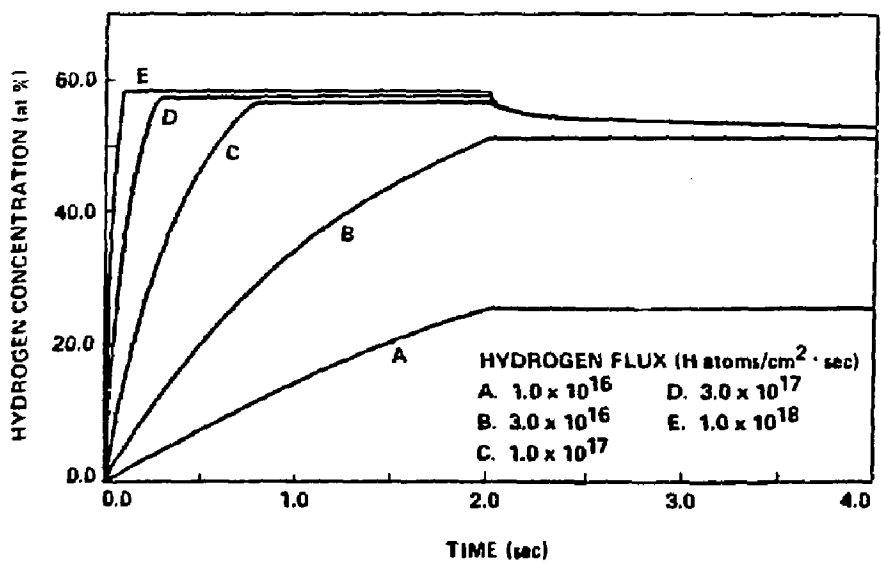
HYDROGEN CONCENTRATION (at %)
60.0
40.0
20.0
0.0
E
D
C
B
A
HYDROGEN FLUX (H atoms/cm^2 · sec)
A. 1.0 x 10^{16}
B. 3.0 x 10^{16}
C. 1.0 x 10^{17}
D. 3.0 x 10^{17}
E. 1.0 x 10^{18}
0.0
1.0
2.0
3.0
4.0
TIME (sec)

Fig. 6(b)

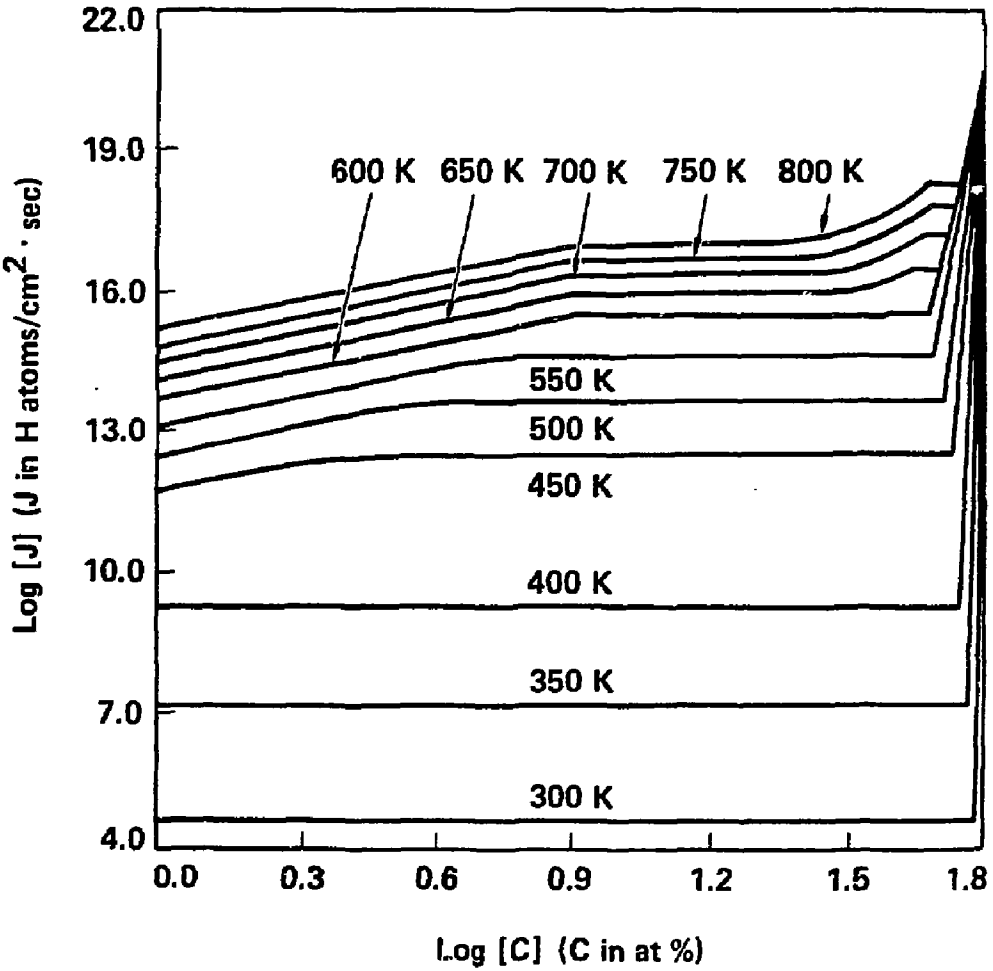
22.0
19.0
16.0
13.0
10.0
7.0
4.0
600 K
650 K
700 K
750 K
800 K
550 K
500 K
450 K
400 K
350 K
300 K
0.0
0.3
0.6
0.9
1.2
1.5
1.8
Log [J] (J in H atoms/cm2 · sec)
Log [C] (C in at %)

Fig. 7

INTERNAL DISTRIBUTION

5731 Boelter Hall

R.J.DiMelfi
K.Kleefeldt
H.Madarame

6288 Boelter Hall-1

M.A.Abdou
N.M.Ghoniem
P.J.Gierszewski
Y.Oyama
M.S.Tillack
M.Z.Youssef

6291 Boelter Hall

K.J.Andrews
R.W.Conn
M.A.Firestone
D.M.Goebel
S.P.Grotz
Y.Hirooka
T.K.Mau
F.Najimabadi
G.C.Pomraning
A.K.Prinja
K.Shin
K.Taghavi

6671 Boelter Hall

L. Keller

2567 Boelter Hall

Z.Lucky
R.Taylor

5532 Boelter Hall

G.Apostolakis
V.Dhir

6531 Boelter Hall

A.Ardell
B.Dunn

6532 Boelter Hall

R.F.Bunshah

7731 Boelter Hall

F.Chen
T.Forrester
C.Joshi

7702 Boelter Hall

N.Luhmann
W.A.Peebles

8270 Boelter Hall

EMS Library-2

1-130 Knudsen Hall

Physics Library-1

J.Dawson
B.Fried
C.Kennel
G.Morales
R.Stenzel
A.Wong

2080 Young Hall

S.Williams

EXTERNAL DISTRIBUTION (IN ADDITION TO UC20)

Prof. D. R. Olander
Dept. of Nuclear Engineering
University of California, Berkeley
Berkeley, CA 94720

Dr. J. R. Bayless
One Space Park (R1/2144)
Redondo Beach, CA 90278

Dr. J. L. Cecchi
Plasma Physics Laboratory
Princeton University
P. O. Box 451
Princeton, NJ 08544

Dr. H. F. Dylla
Plasma Physics Laboratory
Princeton University
P. O. Box 451
Princeton, NJ 08544

Prof. W. A. Jesser
Dept. of Material Science
School of Enigineering and Applied Science
University of Virginia
Charlottesville, VA 22901

Prof. O. K. Harling
Nuclear Reactor Laboratory
Massachusetts Institute of Technology
138 Albany Street
Cambridge, MA 02139

Dr. F. W. Clinard, Jr.
Controlled Thermonuclear Research Division
Los Alamos National Laboratory
P. O. Box 1663
Los Alamos, NM 87545

Dr. J. G. Hoffman
Controlled Thermonuclear Research Division
Los Alamos National Laboratory
P. O. Box 1663
Los Alamos, NM 87545

Prof. G. L. Kulcinski
Dept. of Nuclear Engineering, Rm. 443
University of Wisconsin
Madison, WI 53706

Prof. E. M. Larsen
Chemistry Building
1101 University Avenue
University of Wisconsin
Madison, WI 53706

Dr. J. H. DeVan
Metals and Ceramics Division
Oak Ridge National Laboratory
P. O. Box Y
Oak Ridge, TN 37830

Dr. C. I. H. Ashby
Sandia National Laboratories
Pulsed Power Sciences Directorate
P. O. Box 5800
Albuquerque, NM 87185

Dr. M. E. Malinowski
Sandia National Laboratories
Pulsed Power Sciences Directorate
Albuquerque, NM 87185

Dr. A. Pontau
Sandia National Laboratories
Pulsed Power Sciences Directorate
Albuquerque, NM 87185

Dr. G. R. Hopkins
GA Technologies Inc.
Fusion and Advanced Technology
P. O. Box 85608
San Diego, CA 92138

Prof. P. C. Stangby
University of Toronto
Institute for Aerospace Studies
4925 Dufferin Street, Downsview
Ontario, CANADA M3H5T6

Prof. H. D. Gesser
Dept. of Chemistry
University of Manitoba
Winnipeg, Manitoba CANADA

Dr. G. M. McCracken
Culham Laboratory
United Kingdom Atomic Energy Authority
Abingdon, Oxon. OX14 3DB
UNITED KINGDOM

Dr. S. K. Erents
Culham Laboratory
United Kingdom Atomic Energy Authority
Abingdon, Oxon. OX14 3DB
UNITED KINGDOM

Dr. K. Sone
Japan Atomic Energy Research Institute
Division of Thermonuclear Fusion Research
Plasma Engineering Laboratory
Tokai, Ibaraki, JAPAN 319-11

Dr. M. Saidoh
Japan Atomic Energy Research Institute
Division of Thermonuclear Fusion Research
Plasma Engineering Laboratory
Tokai, Ibaraki, JAPAN 319-11

Dr. S. Okuda
Radiation Center of Osaka Prefecture
Shiuke-cho, Sakai, Osaka

Prof. S. Veprek
Institute of Inorganic Chemistry
Univerisity of Zurich
8057 Zurich, SWITZERLAND

Dr. E. Vietzke
Institut fur Chemie 1
KFA Julich, EURATOM - Association
P. O. B. 1913
D - 517 Julich 1
WEST GERMANY

Dr. J. Roth
Max-Plank-Institut fur Plasmaphysik
EURATOM - Association
D - 8046 Garching, Munchen
WEST GERMANY

Dr. J. Bohdansky
Max-Plank-Institut fur Plasmaphysik
EURATOM - Association
D - 8046 Garching, Munchen
WEST GERMANY

Dr. E. Fromm
Max-Plank-Institut fur Metallforschung
Seetstrasse 92
7000 Stuttgart-1
WEST GERMANY